

PDE-Based Model for Weld Defect Detection on Digital Radiographic Image

Suhaila Abd Halim and Arsmah Ibrahim

Center of Mathematics Studies, Faculty of Computer & Mathematical Sciences, Universiti Teknologi MARA, 40450
Shah Alam, Selangor DE, Malaysia

Email: {suhaila889, arsmah097}@salam.uitm.edu.my

Yupiter HP Manurung

Advanced Manufacturing Technology Center, Faculty of Mechanical Engineering, Universiti Teknologi MARA, 40450
Shah Alam, Selangor DE, Malaysia

Email: yupiter.manurung@salam.uitm.edu.my

Abstract—Partial differential equation (PDE)–based image processing has played a substantial role and become more popular in the recent years. In the application of weld defect detection, the PDE models can be applied for image smoothing and segmentation. In this study, anisotropic diffusion proposed by Perona Malik known as Perona Malik Anisotropic Diffusion (PMAD) model is used as a denoising process for smoothing while level set by Chan and Vese is used as detection process for segmentation. The PMAD model has been solved using Peaceman Rachford (PR) scheme in order to improve the denoising process. A set of radiographic images that contain weld defects are used as input data. The implementation of the algorithm is done using Matlab R2009a. The average error on contour-based metric and CPU times are used to evaluate the accuracy and the efficiency of the CV model and the thresholding method on the proposed denoising process. From the results, the contour detection of weld defect is improved on image after denoising process using CV model as compared with the thresholding. In conclusion, the PDE-based model can be applied in detecting weld defect on radiographic images which could assist radiography inspector in their inspection for an accurate evaluation.

Index Terms—partial differential equation, perona malik anisotropic diffusion, chan vese model, peaceman rachford, thresholding, denoising

I. INTRODUCTION

Digital Radiography (DR) is a nondestructive testing (NDT) technique used in many industrial applications to view and evaluate the quality of an object without destroying its original component. A DR is a filmless radiography that requires less radiation and has the ability to enhance and digitally transfer the image for immediate action to be taken. Consequently this produced significant time savings and higher productivity. DR has been widely used in the welding industry for testing and grading of welds on pressurized piping, pressure vessels, high

capacity storage containers, pipelines and some structural welds.

Radiography inspector is a certified person who is able to identify and trace the existence of defects in the radiographic image based on codes and specifications using manual inspection. But, the manual inspection is time consuming, may produce inconsistent, biased and inaccurate results. Inaccurate results may affect the quality and reliability of the welding component that's being evaluated with the advancement of computer technology, image processing has played an important role in detecting weld defects on welded parts accurately with automated or semi-automated inspection system. The system is aimed to increase the inspection speed, accuracy and reduce the subjectivity of manual inspection results. Halim *et al.* [1] review some of the automated inspection processes in the welding industry.

Automatic or semi-automated inspection is able to produce accurate and reliable results with measurement that could support the radiographer's results. Normally, automated inspection includes the processes of image enhancement, image segmentation, features extraction and image classification. In this study, the processes of image enhancement, image segmentation and feature extraction are discussed.

Image enhancement is a process to restore and enhance the interpretation of information in the image for better visualization and analysis. The process aims to reduce noise and improve the image contrast as normally raw image contains noise or less contrast. In order to reduce or remove the existence of noise and improve the image contrast, several techniques had been applied. Vij and Singh [2] provides a review of image enhancement that can be categorized to point operations, spatial operations, transform operations and pseudo coloring methods. The image enhancement offers an important role as most of the images suffers from poor contrast. Zhu and Huang [3] proposed an improved median filtering with average filtering that could reduce the noise effect and time complexity compared with a standard median filter algorithm.

In the last decades, many mathematical approaches based on partial differential equations (PDEs) have been used in image processing [4]. The algorithm solves the initial value problem for some PDEs for a given amount of time. Anisotropic diffusion is one of PDE-based method that has gained a lot of attention for image restoration and smoothing [5].

Anisotropic diffusion is widely used as edge detection, image restoration, image smoothing and texture segmentation. The anisotropic diffusion was proposed by Perona Malik in 1990. In this study, the Perona Malik Anisotropic Diffusion (PMAD) gives denoising effect which helps in preserving the boundary information of the image. In order to extract the boundary contour, segmentation is explored.

Image segmentation is a difficult task in image processing and still an unsolved problem due to a variety of techniques available that suitable for different applications. Rathod and Anand [6] did a comparative study of image segmentation techniques using morphological edge based, region growing and multistage watershed segmentation techniques in detecting weld defects in order to determine the most accurate detection technique for a different type of defects. They concluded that certain defect can only be detected successfully by specific segmentation technique only.

Thresholding is one the oldest segmentation technique that is widely used because it is easy and computationally inexpensive to be applied [7]. Thiruganam *et al.* [8] combined the global and local thresholding with the Gaussian filtering as noise removal to improve the efficiency of the defect counting method applied on weld image.

The PDEs also provides a good segmentation techniques in which the evolution of curve and surface or image are handled by PDEs. Level set is one of PDE-based methods developed by Osher and Sethian (1988) [9]. Due to the stability and irrelevancy of the level set, it's able to solve problems of corner point, curve breaking and combing [10]. While, level set based on the Chan Vese (CV) model is a new functional from Mumford and Shah. The CV model is able to detect the interior contour by using only an initial curve [10].

Li *et al.* [11] proposed a novel level set method that's been applied to MRI images with intensity inhomogeneous. The proposed method is robust to initialization, faster and more accurate compared with the well known piecewise smooth model.

The feature extraction is used to extract features from images that can be used in recognizing the defects. Shafeek *et al.* [12], [13] calculated the area, perimeter, width and height as defect information for defect identification. Relevant features are important to guarantee the accuracy of recognition process.

In this study, the main improvement of the technique is to use the discretization of PMAD model using Peaceman Rachford (PR) with Chan Vese Level set to detect the weld defect on digital radiographic images.

II. PERONA MALIK ANISOTROPIC DIFFUSION

Perona and Malik (1990) [14] had introduced a new definition of scale space technique and a class of algorithms that realize it was using a diffusion process. The diffusion coefficient is assumed to be a constant for the isotropic diffusion that reduced the image noise while blurred the edges. The Perona and Malik replaced the constant diffusion with diffusion function in order to solve the isotropic diffusion.

The PMAD model has been proven to be effective as a denoising tool [15], [16], [17]. Furthermore, denoising is directly related to image visual quality. Equation (1) is the general representation of anisotropic diffusion by modifying an image via PDE.

$$\frac{\partial}{\partial t} I(x, y, t) = \nabla [c(x, y, t) \nabla I(x, y, t)] \quad (1)$$

Equation (1) can be re-expressed as (2)

$$\frac{\partial}{\partial t} I(x, y, t) = \left[c(x, y, t) \frac{\partial^2}{\partial x^2} I(x, y, t) + c(x, y, t) \frac{\partial^2}{\partial y^2} I(x, y, t) \right] \quad (2)$$

where $I(x, y, t)$ is the gray level at iteration t , ∇ is the divergence operator, $c(x, y, t)$ is the diffusion coefficient function and $\nabla I(x, y, t)$ is the gradient of the image.

The anisotropic diffusion model proposed by Perona and Malik for image denoising has developed as a commonly used filtering technique for noise disturbance alleviation process of ultrasound medical image processing [16]. For the high number of diffusion iteration, the edge of the image features was diffused and further decreased the image quality. The diffusion constant determines the value that triggers the smoothing process. High value of diffusion coefficient treats only very large gradient as edge depending on how high diffusion coefficient is. On the contrary, low value of diffusion coefficient treats even small gradient difference as edge and therefore become a smoothing filter.

III. PMAD BASED ON PR

Peaceman Rachford (PR) is one of the alternating direction implicit (ADI) finite difference scheme. The approximation to (2) given by PR (ADI) scheme is obtained from the modification of Crank-Nicolson scheme [18].

$$\begin{aligned} & \left(1 - \frac{1}{2} \mu_x [c(x, y, t) \delta_x^2] \right) \left(1 - \frac{1}{2} \mu_y [c(x, y, t) \delta_y^2] \right) I_{i,j}^{n+1} \\ & = \left(1 + \frac{1}{2} \mu_x [c(x, y, t) \delta_x^2] \right) \left(1 + \frac{1}{2} \mu_y [c(x, y, t) \delta_y^2] \right) I_{i,j}^n \end{aligned} \quad (3)$$

By introducing the intermediate level of $n+1/2$ and level $n+1$, (3) becomes:

$$\left(1 - \frac{1}{2} \mu_x [c(x, y, t) \delta_x^2] \right) I_{i,j}^{n+1/2} = \left(1 + \frac{1}{2} \mu_y [c(x, y, t) \delta_y^2] \right) I_{i,j}^n \quad (4)$$

$$\left(1 - \frac{1}{2}\mu_y [c(x, y, t)\delta_y^2]\right) I_{i,j}^{n+1} = \left(1 + \frac{1}{2}\mu_x [c(x, y, t)\delta_x^2]\right) I_{i,j}^{n+1/2} \quad (5)$$

The ADI method is known to be very efficient in solving diffusion equations [19]. By computing level $n+1/2$, (4) can be elaborated to (6).

$$\begin{aligned} & [1 + \mu_x c(x, y, t)] I_{i,j}^{n+1/2} + \left[-\frac{1}{2}\mu_x c(x, y, t)\right] I_{i+1,j}^{n+1/2} + \left[-\frac{1}{2}\mu_x c(x, y, t)\right] I_{i-1,j}^{n+1/2} \quad (6) \\ & = [1 - \mu_y c(x, y, t)] I_{i,j}^n + \left[\frac{1}{2}\mu_y c(x, y, t)\right] I_{i,j+1}^n + \left[\frac{1}{2}\mu_y c(x, y, t)\right] I_{i,j-1}^n \end{aligned}$$

And at level $n+1$, the (5) also can be expanded to (7).

$$\begin{aligned} & [1 + \mu_y c(x, y, t)] I_{i,j}^{n+1} + \left[-\frac{1}{2}\mu_y c(x, y, t)\right] I_{i,j+1}^{n+1} + \left[-\frac{1}{2}\mu_y c(x, y, t)\right] I_{i,j-1}^{n+1} \quad (7) \\ & = [1 - \mu_x c(x, y, t)] I_{i,j}^{n+1/2} + \left[\frac{1}{2}\mu_x c(x, y, t)\right] I_{i+1,j}^{n+1/2} + \left[\frac{1}{2}\mu_x c(x, y, t)\right] I_{i-1,j}^{n+1/2} \end{aligned}$$

where $\mu_x = \mu_y$ is the rate of diffusion, $I_{i,j}^n$ is the image in i^{th} and j^{th} location for n^{th} level and $c(x, y, t)$ is the diffusion coefficient function which can be defined as in (8).

$$c(x, y, t) = e^{(-\|\nabla I(x, y, t)\|/K)^2} \quad (8)$$

where $\nabla I(x, y, t)$ is the image gradient and K is the contrast parameter that allows differences of large gradient values with weak gradient values on image.

IV. CHAN VESE LEVEL SET

CV Model is an active contour model that was proposed by Chan and Vese in 2001 [20]. It is based on Mumford-Shah functional that is able to detect objects without gradient boundaries. CV defined the energy $F(c_1, c_2, C)$ as in (9) [21].

$$\begin{aligned} F(c_1, c_2, C) &= \mu \cdot \int \delta(C) |\nabla C| dx dy + v \cdot \int Heaviside(C) dx dy \\ &+ \lambda_1 \int_{inside(C)} |f(x, y) - c_1|^2 dx dy \quad (9) \\ &+ \lambda_2 \int_{outside(C)} |f(x, y) - c_2|^2 dx dy \end{aligned}$$

where values of μ , v , λ_1 and λ_2 are positive constant parameters. c_1 is the intensity inside boundary curve C where else c_2 is the intensity outside C of image $I(x, y)$. The c_1 (10) and c_2 (11) can be updated at each iteration.

$$c_1 = \frac{\int f(x, y) \cdot H(C(x, y)) dx dy}{\int H(C(x, y)) dx dy} \quad (10)$$

And

$$c_2 = \frac{\int f(x, y) \cdot (1 - H(C(x, y))) dx dy}{\int (1 - H(C(x, y))) dx dy} \quad (11)$$

In which the $H(C(x, y))$ is the heaviside function that can be defined as:

$$H(C) = \frac{1}{2} \left[1 + \frac{2}{\pi} \arctan\left(\frac{C}{\epsilon}\right) \right] \quad (12)$$

And the dirac delta is:

$$\delta(C) = H'(C) = \frac{1}{\pi} \frac{\epsilon}{\epsilon^2 + C^2} \quad (13)$$

Then, the (9) can be solved using Euler Lagrange equation,

$$\frac{\partial C}{\partial t} = \delta(C) \left[\mu \operatorname{div} \left(\frac{\nabla C}{|\nabla C|} \right) - (f(x, y) - c_1)^2 + (f(x, y) - c_2)^2 \right] \quad (14)$$

where $\operatorname{div} \left(\frac{\nabla C}{|\nabla C|} \right)$ is the curvature. The $\frac{\partial C}{\partial t}$ can be numerically expressed as explicit scheme of (15).

$$C_{i,j}^{n+1} = C_{i,j}^n + \delta(C) \Delta t \begin{bmatrix} \mu \operatorname{div} \left(\frac{\nabla C}{|\nabla C|} \right) \\ -(f(x, y) - c_1)^2 \\ +(f(x, y) - c_2)^2 \end{bmatrix} \quad (15)$$

The detail formulation of the CV model can be referred in [20].

V. METHODOLOGY

The implementation of the experiment uses MATLAB R2009a. Table I shows the detection algorithm of weld defect on digital radiographic images.

TABLE I. DETECTION ALGORITHM

Initialization: Image $I(x, y)$, number of iterations t_1, t_2
Phase 1: Image acquisition and define region of interest (ROI)
Phase 2: Image denoising using the PMAD with PR Median filtering on $I(x, y)$ for $i=1$ to t_1 Define image gradient Determine diffusion coefficient, $c(x, y, t)$ Compute (6) for level $n+1/2$ Compute (7) for level $n+1$ end
Phase 3: Application of the CV model Determine initial contour for $i=1$ to t_2 Calculate c_1 and c_2 Compute (15) end
Phase 4: Extract features outline
Phase 5: Performance evaluation

A. Phase 1: Image Acquisition and Define Region of Interest

The process of image acquisition is explained in [22]. From the acquired digital image, the image ROI is defined in the suspected areas of defects in order to reduce the processing time and avoid detecting the false defect.

B. Phase 2: Image Denoising Using PMAD with PR

In applying the PDE model, the initial condition (IC) and boundary conditions (BC) are determined. The IC is defined as:

$$I(x, y, 0) = S \quad 0 < x < X, \quad 0 < y < Y$$

where S represents the intensity value of original image (I_o), $S \in Z^+$, $0 \leq S \leq 255$ for grayscale image.

while the BC is based on dirichlet boundary condition that defined as:

$$I(0, y, t) = I(X, y, t) = 0, \quad 0 < y < Y, t > 0$$

$$I(0, x, t) = I(x, Y, t) = 0, \quad 0 < x < X, t > 0$$

By applying (6) and (7), the application of the denoising process produced the processed image (I_p). For each iteration, t_1 the values $\mu = 0.1$ and $K=200$ are the best choice among various options from the random simulation done.

C. Phase 3: Chan Vese Level Set

In applying Chan Veset Level set, the values of $\mu = 0.1$, $dt = 0.1$, $\lambda_1 = \lambda_2 = 1$ and $\varepsilon = 10^{-5}$ are set to be implemented.

The result from denoising process in *Phase 2* is determined as $I(x,y)$ that need to be used in (15). After applying the initial contour and after iteration, t_2 then the final contour of defect on image is produced.

D. Phase 4: Features Extraction

In this study, two features of weld defect are calculated that are the area and perimeter. The calculation of the area and perimeter can be referred in [23].

E. Phase 5: Performance Evaluation

The segmentation results of weld defects are evaluated using the average error, $e_{average}(C)$ on contour-based metric in which for each point, $P_i, i=1, \dots, N$ on the contour C , the error is calculated as:

$$e_{average}(C) = \frac{1}{N} \sum_{n=1}^N dist(P_i, Q_i) \quad (16)$$

The $e_{average}(C)$ computed the average distance of point P_i to the ground truth contour, Q_i . The ground truth contour is the contour of the true object boundary that is defined by radiography inspector. Then, the contour is extracted using CV and thresholding (*thresh*) techniques are used as comparison with the contour of ground truth.

Besides the average error, the processing time also computed in order to measure the efficiency of the technique based on CPU times.

VI. RESULTS AND DISCUSSION

The discretized scheme of PMAD with PR is implemented on several samples of digital radiographic images that contain defects. Fig. 1 shows the five samples

of the I_o and the I_p after denoising process using the scheme.

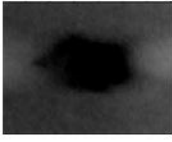
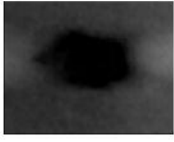
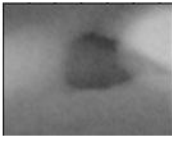
Image	I_o	I_p
I_1		
I_2		
I_3		
I_4		
I_5		

Figure 1. Five samples of original image (I_o) and processed image (I_p).

It can be seen that the I_p produced a clearer and smoother effect on image than I_o due to the smoothing effect of the anisotropic diffusion.

Fig. 2 presents the results for a digital radiographic image of weld defect with the curve evolution processes at different iteration, t_2 .

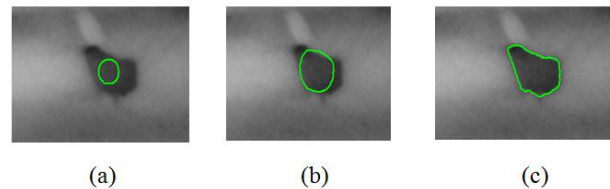


Figure 2. Weld defect detection with curve evolution processes (a) Initial Contour (b) Intermediate Contour (c) Final Contour.

For these sample images, the detection results are depicted in Fig. 3. For the detection of I_p using CV, the result of contour detection is better compared with detection using thresholding (*thresh*) except for the I_5 .

Fig. 4 shows the graph of $e_{average}(C)$ for the CV and thresh after implementing proposed denoising method on the five samples of images. The $e_{average}(C)$ indicates the accuracy of a technique as compared with the ground truth as a benchmark.

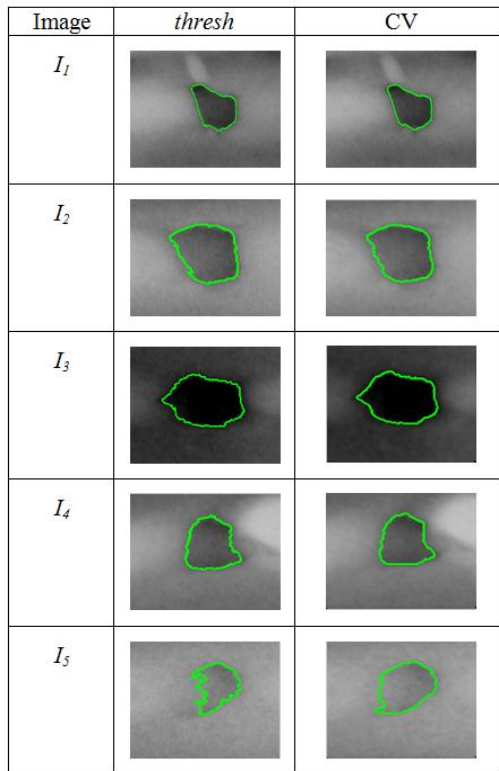


Figure 3. Final contour of weld defect detection on the sample images.

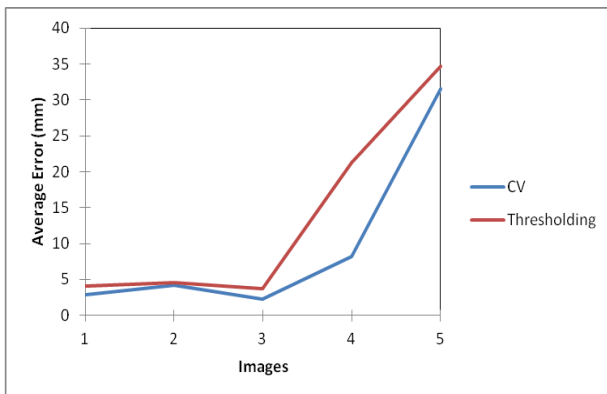


Figure 4. The accuracy of the CV and thresholding after the proposed denoising scheme.

The CV provides better accuracy as compared with thresh. The error for I_5 is quite high due to the lack of contrast between the defect and the background of the image which make the contour detection of the defect becomes difficult and less accurate compared to the ground truth contour.

In determining the efficiency of a technique, the CPU times to run each process is completed. Fig. 5 demonstrates the graph of CPU times in applying the CV and thresh on the I_p . From the graph, the CPU times of the CV indicate much faster in processing time than the thresh. Besides that, the determination of the threshold value in thresholding is a crucial part in which incorrect value produced incorrect contour detection. Hence CV is an efficient technique compared to thresh.

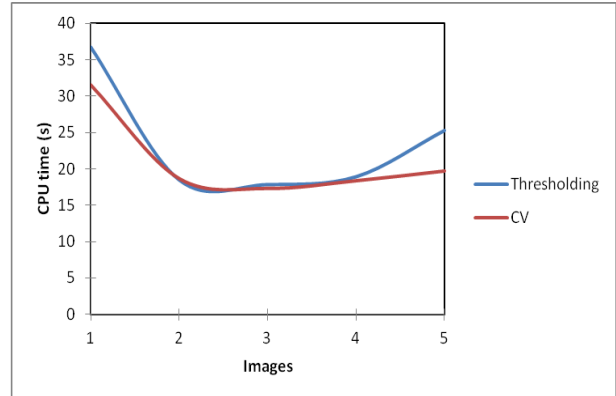


Figure 5. CPU times (s) on sample images.

Table II tabulates the features that have been calculated using both methods. It can be seen that on the average, the calculated values of CV are close to the ground truth values compared with the features using thresh values.

TABLE II. FEATURE EXTRACTION

Image	Feature	Ground truth	thresh	CV
I_1	Area (mm^2)	173.5	198.5	174.6
	Perimeter (mm)	13.2	14.84	13.36
I_2	Area (mm^2)	153.7	154.5	140.6
	Perimeter (mm)	11.26	12.64	11.35
I_3	Area (mm^2)	159.5	185.7	160.2
	Perimeter (mm)	12.42	13.71	12.41
I_4	Area (mm^2)	106.8	106.5	106.2
	Perimeter (mm)	9.714	12.11	10.08
I_5	Area (mm^2)	184.4	151.8	135.4
	Perimeter (mm)	12.84	15.16	12.35

As a continuation from Table II, the percentage error for area and perimeter are calculated and tabulated in Table III. From the results, the CV produced less error compared with thresh except for the areas for I_2 and I_5 . This also indicates a better performance in terms of features error.

TABLE III. PERCENTAGE ERROR OF FEATURES

Image	% error			
	Area (mm^2)		Perimeter (mm)	
	thresh	CV	thresh	CV
I_1	14.4092	0.634	12.4242	1.2121
I_2	0.5205	8.5231	12.2558	0.7993
I_3	16.4263	0.4389	10.3865	0.0805
I_4	0.2809	0.5618	24.6654	3.7678
I_5	17.679	26.5727	18.0685	3.8162

VII. CONCLUSION

The application of modified PMAD model with PR scheme as denoising process plays a significant role in

detecting weld defects in digital radiographic images. By combining the model with the CV, the results provide a better performance of detection in terms of accuracy and efficiency instead of using thresholding as compared to the ground truth contour. The proposed method allows the radiography inspector to produce accurate and consistent weld defect inspection result.

ACKNOWLEDGMENT

This work was supported in part by a grant from the Ministry of Higher Education Malaysia (MOHE). The authors also would like to express their gratitude to Mr. Shahidan Mohamad, senior technician at the Laboratory of Advanced Manufacturing, Faculty of Mechanical Engineering, Universiti Teknologi MARA (UiTM), Shah Alam for the technical support during this work.

REFERENCES

[1] S. A. Halim, A. Ibrahim, and Y. H. P. Manurung, "A review on automated inspection and evaluation system of weld defect detection on radiographic image," *International Journal of Recent Scientific Research*, vol. 3, no. 12, pp. 1019-1023, December 2012.

[2] K. Vij and Y. Singh, "Comparison between different techniques of image enhancement," *International Journal of VLSI and Signal Processing Applications*, vol. 1, no. 2, pp. 112-117, May 2011.

[3] Y. Zhu and C. Huang, "An improved median filtering algorithm combined with average filtering," in *Proc. 2011 3rd International Conference on Measuring Technology and Mechatronics Automation*, Shanghai, 2011, pp. 420-423.

[4] S. Angenent, E. Pichon, and A. Tannenbaum, "Mathematical methods in medical image processing," *Bulletin (New Series) of The American Mathematical Society*, vol. 43, no. 3, pp. 365-396, July 2006.

[5] A. B. Kazmi, K. A. Agrawal, and V. Upadhyay, "Image enhancement processing using anisotropic diffusion," *International Journal of Computer Science Engineering and Information Technology Research*, vol. 3, no. 1, pp. 293-300, March 2013.

[6] V. R. Rathod and R. S. Anand, "A comparative study of different segmentation techniques for detection of flaws in NDE weld images," *Journal of Nondestructive Evaluation*, vol. 31, no. 1, pp. 1-16, October 2011.

[7] P. Thakare, "A study of image segmentation and edge detection techniques," *International Journal on Computer Science and Engineering*, vol. 3, no. 2, pp. 899-904, February 2011.

[8] M. Thiruganam, S. M. Anouncia, and S. Kantipudi, "Automatic defect detection and counting in radiographic weldment images," *International Journal of Computer Applications*, vol. 10, no. 2, pp. 1-5, November 2010.

[9] S. Osher and J. Sethian, "Fronts propagating with curvature-dependent speed: Algorithms based on Hamilton-Jacobi formulations," *Journal of Computational Physics*, vol. 79, no. 1, pp. 12-49, November 2008.

[10] X. Jiang, R. Zhang, and S. Nie, "Image segmentation based on pdes model: A survey," in *Proc. 3rd International Conference on Bioinformatics and Biomedical Engineering*, Beijing, 2009, pp. 1-4.

[11] C. Li, C. Xu, C. Gui, and M. D. Fox, "Distance regularized level set evolution and its application to image segmentation," *IEEE Transactions on Image Processing*, vol. 19, no. 12, pp. 3243-3254, December 2010.

[12] H. I. Shafeek, E. S. Gadelmawla, A. A. Abdel-Shafy, and I. M. Elewa, "Assessment of welding defects for gas pipeline radiographs using computer vision," *NDT & E International*, vol. 37, no. 4, pp. 291-299, 2004.

[13] H. I. Shafeek, E. S. Gadelmawla, A. A. Abdel-Shafy, and I. M. Elewa, "Automatic inspection of gas pipeline welding defects using an expert vision system," *NDT & E International*, vol. 37, no. 4, pp. 301-307, 2004.

[14] P. Perona and J. Malik, "Scale-space and edge detection using anisotropic diffusion," *IEEE Transactions on Pattern Analysis and Machine Intelligence*, vol. 12, no. 7, pp. 629-639, July 1990.

[15] P. Guidotti and K. Longo, "Two enhanced fourth order diffusion models for image denoising," *Journal of Mathematical Imaging and Vision*, vol. 40, no. 2, pp. 188-198, January 2011.

[16] K. W. Lai, Y. C. Hum, and S. Eko, "Computerized anisotropic diffusion of two dimensional ultrasonic images using multi-direction spreading approaches," *Journal on Biology and Biomedicine*, vol. 8, no. 3, pp. 102-110, July 2011.

[17] S. M. Chao and D. M. Tsai, "An improved anisotropic diffusion model for detail and edge-preserving smoothing," *Journal on Pattern Recognition*, vol. 31, no. 13, pp. 2012-2023, October 2010.

[18] K. W. Morton and D. F. Mayer, *Numerical Solution of Partial Differential Equations*, 2nd ed. Cambridge University Press: New York, 2005, ch. 2.

[19] Y. J. Cha and S. J. Kim, "Edge-forming methods for color image zooming," *IEEE Transactions on Image Processing*, vol. 15, no. 8, pp. 2315-2323, August 2006.

[20] T. F. Chan and L. A. Vese, "Active contours without edges," *IEEE Transactions on Image Processing*, vol. 10, no. 2, pp. 266-277, February 2001.

[21] H. Xu and X. F. Wang, "Automated segmentation using a fast implementation of the Chan-Vese models," *Advanced Intelligent Computing Theories and Applications. With Aspects of Artificial Intelligence*, no. 5227, pp. 1135-1141, 2008.

[22] S. A. Halim, A. Ibrahim, M. I. Jayes, and Y. H. P. Manurung, "Weld defect features extraction on digital radiographic image using chan vese model," in *Proc. 9th IEEE Colloquium on Signal Processing & Its Applications*, Kuala Lumpur, Malaysia, 2013, pp. 67-72.

[23] S. A. Halim, N. A. Hadi, A. Ibrahim, and Y. H. P. Manurung, "The geometrical feature of weld defect in assessing digital radiographic image," in *Proc. 2011 IEEE International Conference on Imaging Systems and Techniques*, Pulau Pinang, Malaysia, 2011, pp. 189-193.



Suhaila Abd Halim received the BSc. in Computational Mathematics from Universiti Teknologi MARA, Shah Alam in 2005 and her MSc. In Mathematics from Universiti Sains Malaysia, Pulau Pinang in 2007. She is currently pursuing her PhD in the area of image processing and her research interests include image processing and image watermarking. She is a life member of the Malaysian Mathematical Sciences Society since 2010 and a member of IEEE since 2013.



Arsmah Ibrahim is currently a mathematics Professor at Faculty of Computer and Mathematical Sciences, Universiti Teknologi MARA (UiTM) Malaysia. She received her MSc. (Mathematics) from Northern Illinois University, USA and her PhD (Numerical Analysis) from Universiti Kebangsaan Malaysia. Her research interests include Numerical Analysis and Computational Mathematics.



Yupiter HP Manurung is currently an Associate Professor at Faculty of Mechanical Engineering, Universiti Teknologi MARA (UiTM) Malaysia. He received his BSc. in Manufacturing Technology from University of Applied Sciences GSO Nuernberg, Germany and his MSc. as well as Ph.D in Manufacturing Technology from University O-v-G Magdeburg, Germany. He also obtained International/European/ German Welding Engineer (IWE/EWE/SFI) from SLV Halle, Germany and Laser Technology from University Jena, Germany. His research interests include Advanced Manufacturing Technology and Simulation, Advanced Welding Technology and Simulation, Quality & Reliability Engineering and Digital Radiography.